Atlas Journal of Materials Science 1 (1): 1–11, 2014
doi: 10.5147/ajms.2014.0168

Phase Equilibria at Ti–Al Interface Under Low Oxygen Pressure

Chien Chon Chen

Department of Energy Engineering, National United University, Miaoli 36003, Taiwan

Received: October 17, 2013 / Accepted: December 20, 2013

Abstract

In this paper, thirty-nine phases in the Ti-Al-O system at high temperatures have been analyzed through thermodynamic calculations. A Ti-Al-O isothermal stability diagram was obtained from the thermochemical data. The diagrams described the equations for Ti/Al intermetallic compounds at Al_2O_3/Ti_xAl_y and $Al_2O_3/TiAl_2O_5$ interfaces, and their corresponding regions. Four univariant equilibria points and ten bivariant equilibria lines at 1000 K were obtained. The equations for the coexistence points and interface lines were also obtained. A three-domain diagram of Ti-Al-O phase arrangement at temperatures between 1000 K and 1200 K was shown. Thermodynamic calculations confirmed that the formation of titanium aluminate spinel ($TiAl_2O_5$) requires a threshold TiO_2 activity and a partial pressure of oxygen. In the Ti-Al-O system, when $a_{TiO2} < 0.121$ and $\log P_{O2} < -47.2$ atm, $TiAl_2O_5$, TiO_2, and Al_2O_3 compounds are not formed at 1000 K; while at the Ti/Al interfaces, compounds are formed in the order of $Ti_3Al_{(s)} \rightarrow TiAl_{(s)} \rightarrow TiAl_{2(s)} \rightarrow TiAl_{3(s)}$.

Keywords: Ti-Al-O, isothermal stability diagram, partial pressure, intermetallic compounds, thermodynamics.

* Corresponding author: chentexas@gmail.com

Introduction

Titanium-aluminide compounds, known as ordered intermetallic compounds, are potential candidates for elevated temperature applications in the aerospace and automotive industries because of their light weight, high specific strength, high specific modulus, and good creep resistance (Chen et al., 2009; Zhong et al., 2012; Wang et al., 2013).The intermetallic compounds of Ti-Al alloys include Ti_3Al, TiAl, $TiAl_2$, and $TiAl_3$ (Charlu et al., 1974; Chen et al., 1995; Braun et al., 2001). They possess attractive properties of relatively low density, high melting point, high thermal conductivity, high specific strength, and resistance to oxidation at elevated temperatures. The Ti-Al alloys, with a duplex (Ti_3Al+TiAl) lamellar microstructure, exhibited improved room-temperature ductility while maintaining adequate high-temperature creep rates and oxidation resistance (Ward-Close et al., 1995; Lin et al., 2000; Cheng et al., 2013).

Ti/Al_2O_3 interface reactions have been extensively investigated in the literature (Lu et al., 1995a; Lu et al., 1995b; Dehm et al., 1998; Zalar et al., 1999; Feng et al., 2012). However, some controversies remained about the mechanism and formation sequence of the interface reaction products, since different experimental constructions may affect both thermodynamic and kinetic conditions and thus the diffusion path in the Ti-Al-O system. For example, Li (Li et al., 1992) suggested two possible diffusion paths at 1100 °C: $Al_2O_3/TiAl/Ti_3Al/\alpha$-Ti/β-Ti, for an infinite Ti supply from thick Ti foils; or $Al_2O_3/Ti_3Al/\alpha$-Ti/β-Ti, for a finite Ti supply from thin Ti foils. Additionally, the oxides of TiO_2 and $TiAl_2O_5$ could be formed in the Ti-Al system. Their formation depends on the partial pressure of oxygen and the activity of titanium. The mechanisms of formation of the titanium aluminate spinel ($TiAl_2O_5$) in the TiO_2-Al_2O_3 interface under 1 bar oxygen partial pressure have been investigated in Seifert's studies (Seifert et al., 2001). Xu et al. (2006) found that $TiAl_3$, Ti_2Al_5, $TiAl_2$, TiAl, and Ti_3Al could be formed by a Ti/Al diffusion

couple experimental process. Cai et al. (2006) fabricated Al/TiO_2, Ti(Al,O)/Al_2O_3, $Ti_3Al(O)/Al_2O_3$ and $TiAl/Al_2O_3$ composites by high energy mechanical milling using Al, TiO_2, Ti, and Al_2O_3 powders as the starting materials.

According to the literature (Kainuma et al., 1994; Gerasimov et al., 1996; Kostov et al., 2008; Pang et al., 2013), several parameters influence Ti/Al interface conditions, such as temperature, partial pressure of oxygen, activity of Ti, activity of compounds, Gibbs free energy, activation energy, heat treatment time, and diffusion coefficient. A convenient method of representing the thermodynamic information involves the construction of isothermal diagrams showing the range of gas compositions, over which a condensed phase can exist either by itself or in equilibrium with another condensed phase. This type of diagram is called an isothermal stability diagram. It can be more useful to apply an isothermal stability diagram in discussing gas-condensed phases at a constant temperature, rather than a general phase diagram of temperature-composition. This work considers the effects of temperature, partial oxygen pressure, activities of Ti and TiO_2, and Gibbs free energy for thermodynamic calculations the Ti-Al-O system. The mechanisms that operate in the Ti-Al-O system at high temperatures are thereby clarified. The purpose of the present work is to explain and locate the compounds in Ti-Al-O system by an isothermal stability diagram, which provides guidelines to obtain titanium-aluminide compounds.

Thermodynamic Calculations and Results

Phases in the Ti-Al-O System

In order to simplify the calculation and the final diagram we ignore the dominant phase in the Ti-O system (TixOy) which has a non-stoichiometry. The phase diagrams (Figure 1) of Al-O (Wriedt, 1985; Copland, 2006), Ti-O, Ti-Al, and TiO_2-Al_2O_3 (Caron et al., 1996), and thermodynamic data books (Pourbaix, 1974; Chase et al., 1985; Barin, 1989) show 31 different condensed phases and 8 gaseous phases in the Ti-Al-O system. The 39 phases are as follows: Al(l), $Al_{(g)}$, $Ti_{(\alpha)}$, $Ti_{(\beta)}$, $Ti_{(g)}$, $O_{2(g)}$, $Al_2O_{3(\alpha)}$), $Al_2O_{3(\kappa)}$, $Al_2O_{3(\delta)}$, $Al_2O_{3(\gamma)}$, $Al_2O_{2(g)}$, $Al_2O_{(g)}$, $AlO_{2(g)}$, $AlO_{(g)}$, $TiO_{(g)}$, $TiO_{(\alpha)}$, $TiO_{(\beta)}$, $TiO_{(\gamma)}$, $TiO_{2(s)}$, $Ti_2O_{(s)}$, $Ti_2O_{3(\alpha)}$, $Ti_2O_{3(\beta)}$, $Ti_3O_{(s)}$, $Ti_3O_{2(s)}$, $Ti_3O_{5(\alpha)}$, $Ti_3O_{5(\beta)}$, $Ti_4O_{7(s)}$, $Ti_5O_{9(s)}$, $Ti_6O_{11(s)}$, $Ti_8O_{15(s)}$, $Ti_9O_{17(s)}$, $Ti_{16}O_{31(s)}$, $Ti_{50}O_{99(s)}$, $TiAl_{(s)}$, $TiAl_{2(s)}$, $TiAl_{3(s)}$, $Ti_2Al_{5(s)}$, $Ti_3Al_{(s)}$, and $TiAl_2O_{5(s)}$. Here, the subscripts g, s and represents gas and solid, respectively, and other scubscripts, different phases. To simplify the calculation of phases in Ti-Al-O system, the 7 gaseous species $Al_{(g)}$, $Ti_{(g)}$, $Al_2O_{2(g)}$, $Al_2O_{(g)}$, $AlO_{2(g)}$, $AlO_{(g)}$, and $TiO_{(g)}$ with the exception of oxygen, will be ignored at first because of their low partial vapor pressure within the Al-O and Ti-O systems. Moreover, because the condensed phase $Al_2O_3(\alpha)$ (ΔG = –1361.42 kJ/mol at 1000 K) (Chase et al., 1985) is much more stable, the other 3 alumina phases of $Al_2O_{3(\alpha)}$, $Al_2O_{3(\kappa)}$, $Al_2O_{3(\delta)}$ will also be ignored. In addition, the 13 condensed phases of $TiO_{(\beta)}$, $TiO_{(\gamma)}$, $Ti_2O_{(s)}$, $Ti_2O_{3(\beta)}$, $Ti_3O_{(s)}$, $Ti_3O_{2(s)}$, $Ti_3O_{5(\beta)}$, $Ti_5O_{9(s)}$, $Ti_6O_{11(s)}$, $Ti_8O_{15(s)}$, $Ti_{16}O_{31(s)}$, $Ti_9O_{17(s)}$, and $Ti_{50}O_{99(s)}$ will also be ignored because they are less stable than $TiO_{(\alpha)}$, $TiO_{2(s)}$, $Ti_2O_{3(\alpha)}$, $Ti_3O_{5(\alpha)}$, and $Ti_4O_{7(s)}$ in the Ti-O system. As a result, the Ti-Al-O isothermal stability diagram now only includes 15 condensed phases, i.e., $Al_{(s,l)}$, $Ti_{(\alpha)}$, $Ti_{(\beta)}$, $Al_2O_{3(\alpha)}$, $TiO_{(\alpha)}$, $TiO_{2(s)}$, $Ti_2O_{3(\alpha)}$, $Ti_3O_{5(\alpha)}$, $Ti_4O_{7(s)}$, $TiAl_{(s)}$, $TiAl_{2(s)}$, $TiAl_{3(s)}$, $Ti_2Al_{5(s)}$, $Ti_3Al_{(s)}$, $TiAl_2O_{5(s)}$, and one gas phase of oxygen which will be investigated by thermochemical data and thermodynamic calculations. The 16 phases used for Ti-Al-O isothermal stability diagram construction in the temperature range of 900 to 1200 K are shown in Table 1.

Gaseous Species

As discussed above, gas species other than oxygen were ignored in developing the isothermal stability diagram. However, vapor pressures in the solid and liquid phases are important in Al-O and Ti-O systems at high temperature. We have discussed Ni-Al-O system in a previous paper (Kuo et al., 2009). In this section, we will discuss the reactions in the gas phase in the Ti–O system. The equilibrium partial vapor pressure of titanium and oxygen in $TiO_{(s)}$ can be calculated from the Gibbs free energy as follows:

$$TiO_{(s)} \rightarrow Ti_{(g)} + \frac{1}{2}O_{2(g)}, \quad \Delta G_1^o = 4.97 - \frac{28262.2}{T}(\text{kJ/mol}) \ [26] \qquad (1)$$

The standard molar free energy change in this reaction is given by $\Delta G^0_1 = -RT \times \ln K_1$. Here K_1 can be expressed as:

$$K_1 = \frac{P_{Ti} \cdot (P_{O_2})^{0.5}}{a_{TiO}} \qquad (2)$$

where a_{TiO}, P_{Ti}, and P_{O2} represent the activity of TiO, partial pressure of Ti, and partial pressure of oxygen, respectively. Since the activity of a solid is a unity, the relationship between P_{Ti} and P_{O2} can be represented as:

$$\log P_{O_{2(g)}} = 2(\log K - \log P_{Ti}) \qquad (3)$$

Additionally,

$$\log K = \frac{-\Delta G_1^o}{2.303RT} \qquad (4)$$

In Equ. 4, K and R are two constants; therefore, ΔG^0 is only a function of temperature T. The ΔG^0 can be express as $\Delta G^0 = A + BT$, where A and B are two numerical numbers. Based on the preceding discussion and thermodynamic data books (Pourbaix 1974; Chase et al., 1985; Barin 1989), the vapor pressures of $Ti_{(g)}$ in $Ti_{(s)}$, $TiO_{(g)}$ in $TiO_{(s)}$, $TiO_{(g)}$ in $Ti_3O_{5(s)}$, $TiO_{(g)}$ in $Ti_4O_{7(s)}$, and $TiO_{(g)}$ in $TiO_{2(s)}$ are:

$$Ti_{(s)} \rightarrow Ti_{(g)} \qquad \Delta G_2^o = 464.9 - 0.138T\ (\text{kJ/mol}) \qquad (5)$$

$$TiO_{(s)} \rightarrow TiO_{(g)} \qquad \Delta G_3^o = 43.8 - 0.085T\ (\text{kJ/mol}) \qquad (6)$$

$$Ti_3O_{5(s)} \rightarrow 3TiO_{(g)} + O_{2(g)} \quad \Delta G_4^o = 2581.2 - 0.707T\ (\text{kJ/mol}) \qquad (7)$$

$$Ti_4O_{7(s)} \rightarrow 4TiO_{(g)} + \frac{3}{2}O_{2(g)} \Delta G_5^o = 3568.1 - 0.961\ (\text{kJ/mol}) \qquad (8)$$

$$TiO_{2(s)} \rightarrow TiO_{(g)} + \frac{1}{2}O_{2(g)} \quad \Delta G_6^o = 984.2 - 0.266\ (\text{kJ/mol}) \qquad (9)$$

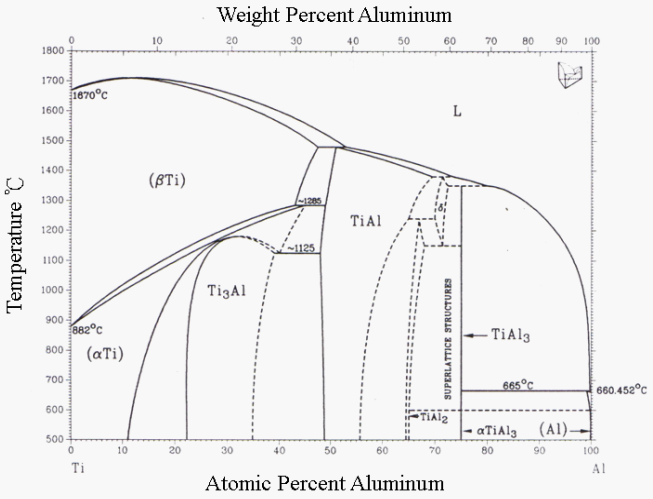

Figure 1(a)

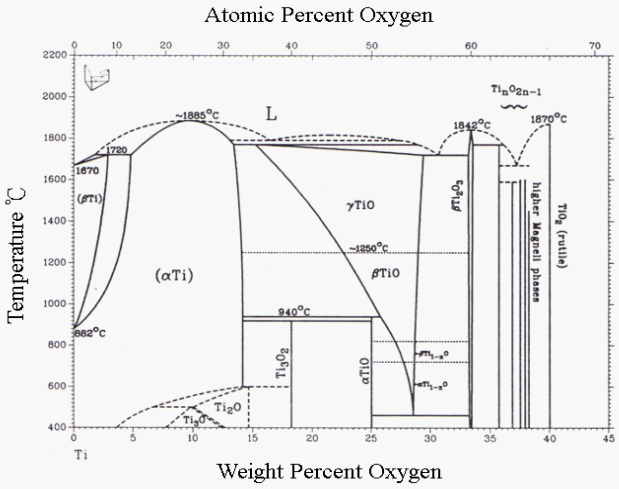

Figure 1(c)

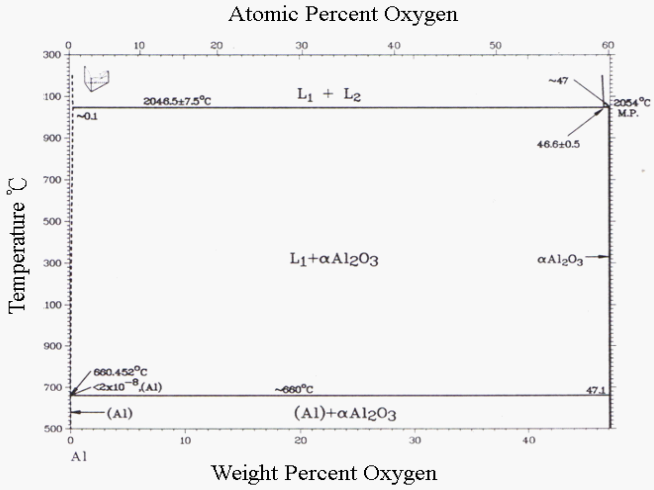

Figure 1(b)

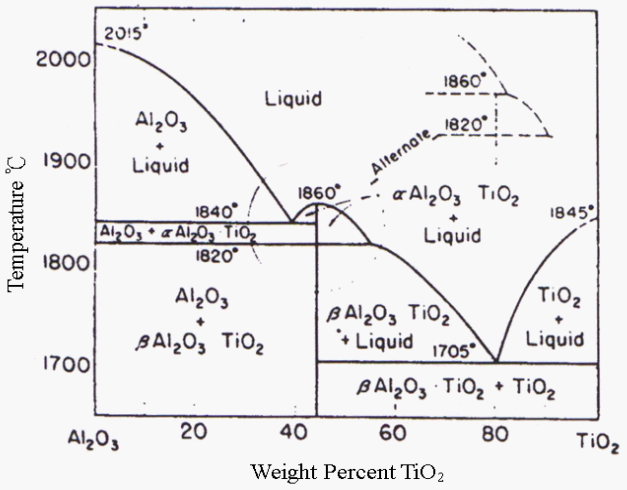

Figure 1(d)

Figure 1. Binary phase diagrams of (a) Ti–Al, (b) Al–O, (c) Ti-O, and (d) Al_2O_3-TiO_2. (Wriedt, 1985; Caron et al., 1996; Copland, 2006).

Table 1. Twenty-three unstable phases can be neglected (deletion line) from the thirty-nine phases of the Ti-Al-O system in a temperature range of 1000 to 1200 K.

$Al_{(s,\ l)}$	~~$Al_{(g)}$~~	$Ti_{(\alpha)}$	$Ti_{(\beta)}$	~~$Ti_{(g)}$~~	$O_{2(g)}$	$Al_2O_{3(\alpha)}$
~~$Al_2O_{3(H)}$~~	~~$Al_2O_{3(\delta)}$~~	~~$Al_2O_{3(\gamma)}$~~	~~$Al_2O_{2(g)}$~~	~~$Al_2O_{(g)}$~~	~~$AlO_{2(g)}$~~	~~$AlO_{(g)}$~~
~~$TiO_{(g)}$~~	$TiO_{(\alpha)}$	~~$TiO_{(\beta)}$~~	~~$TiO_{(\gamma)}$~~	$TiO_{2(s)}$	~~$Ti_2O_{(s)}$~~	$Ti_2O_{3\ (\alpha)}$
~~$Ti_2O_{3\ (\beta)}$~~	~~$Ti_3O_{(s)}$~~	~~$Ti_3O_{2(s)}$~~	$Ti_3O_{5\ (\alpha)}$	~~$Ti_3O_{5\ (\beta)}$~~	$Ti_4O_{7(s)}$	~~$Ti_5O_{9(s)}$~~
~~$Ti_6O_{11(s)}$~~	~~$Ti_7O_{13(s)}$~~	~~$Ti_8O_{15(s)}$~~	~~$Ti_{50}O_{99(s)}$~~	$TiAl_{(s)}$	$TiAl_{2(s)}$	$TiAl_{3(s)}$
~~$Ti_9O_{17(s)}$~~	$Ti_2Al_{5(s)}$	$Ti_3Al_{(s)}$	$TiAl_2O_{5(s)}$			

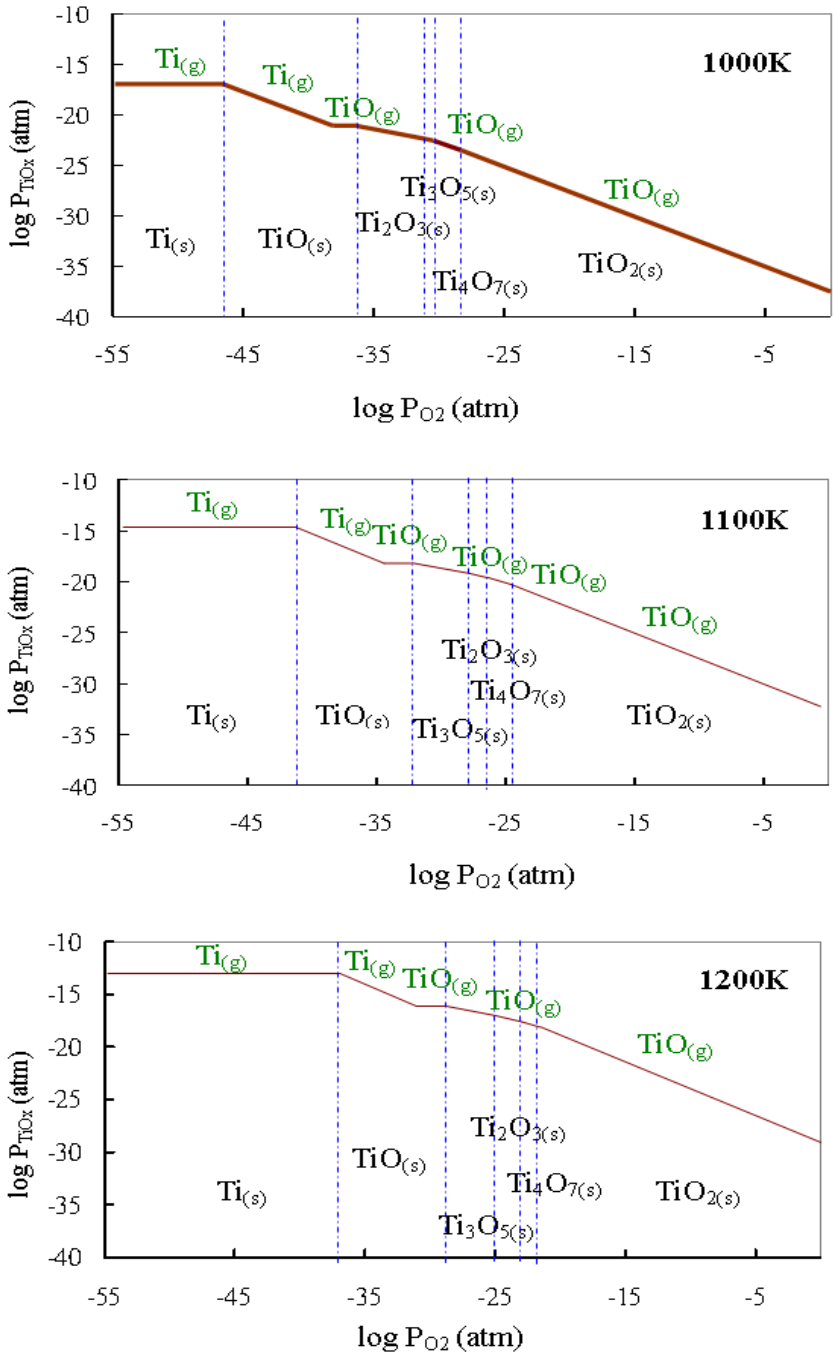

Figure 2. The pressure curves of $Ti_{(g)}$ and $TiO_{(g)}$ in Ti(s) , $TiO_{(s)}$, $Ti_2O_{3(s)}$, $Ti_3O_{5(s)}$, $Ti_4O_{7(s)}$, and $TiO_{2(s)}$ condensed phases at (a) 1000 K, (b) 1100 K, and (c) 1200 K.

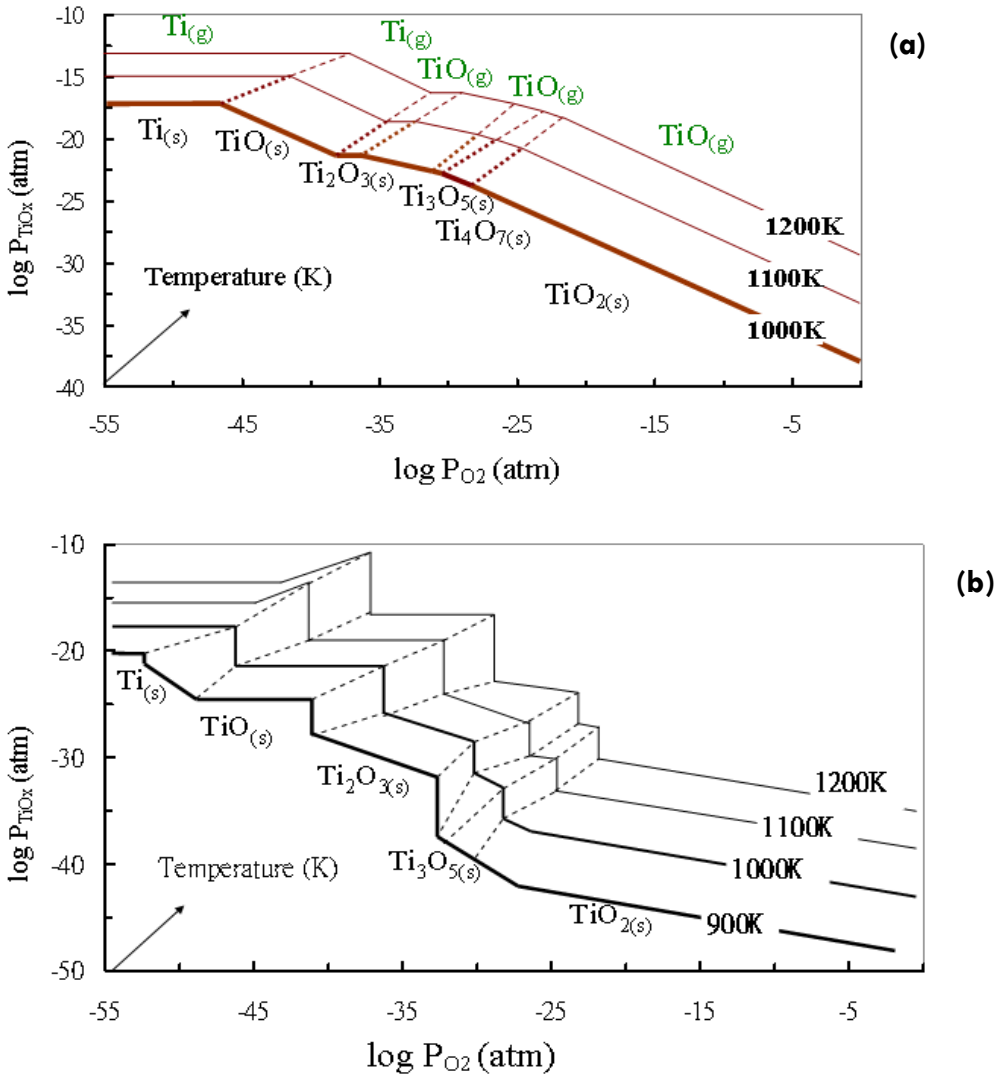

Figure 3. Belted and stepped curves of $Ti_{(g)}$ and $TiO_{(g)}$ dominating the condensed phases of $Ti_{(s)}$, $TiO_{(s)}$, $Ti_3O_{5(s)}$, $Ti_4O_{7(s)}$, and $TiO_{2(s)}$ at temperatures of 900 to 1200 K.

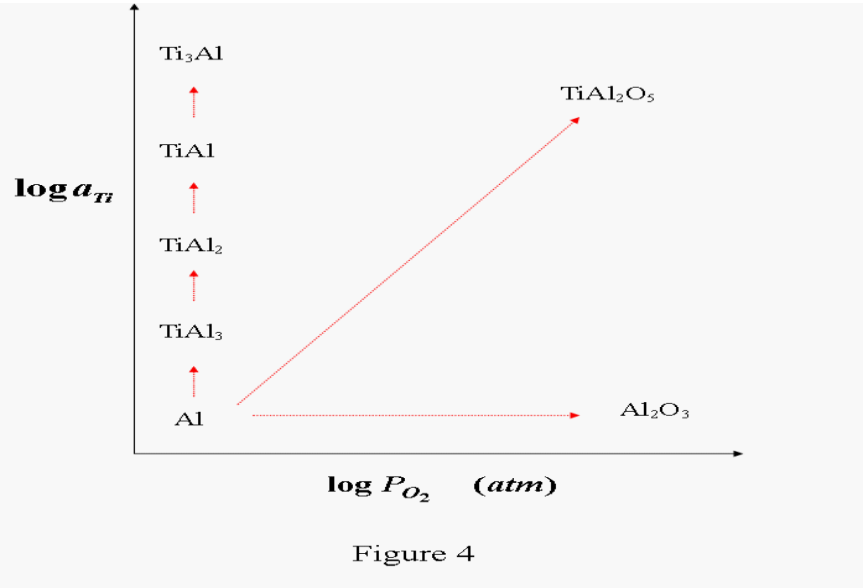

Figure 4. Schematic of Ti-Al-O thermodynamic system in the isothermal stability diagram.

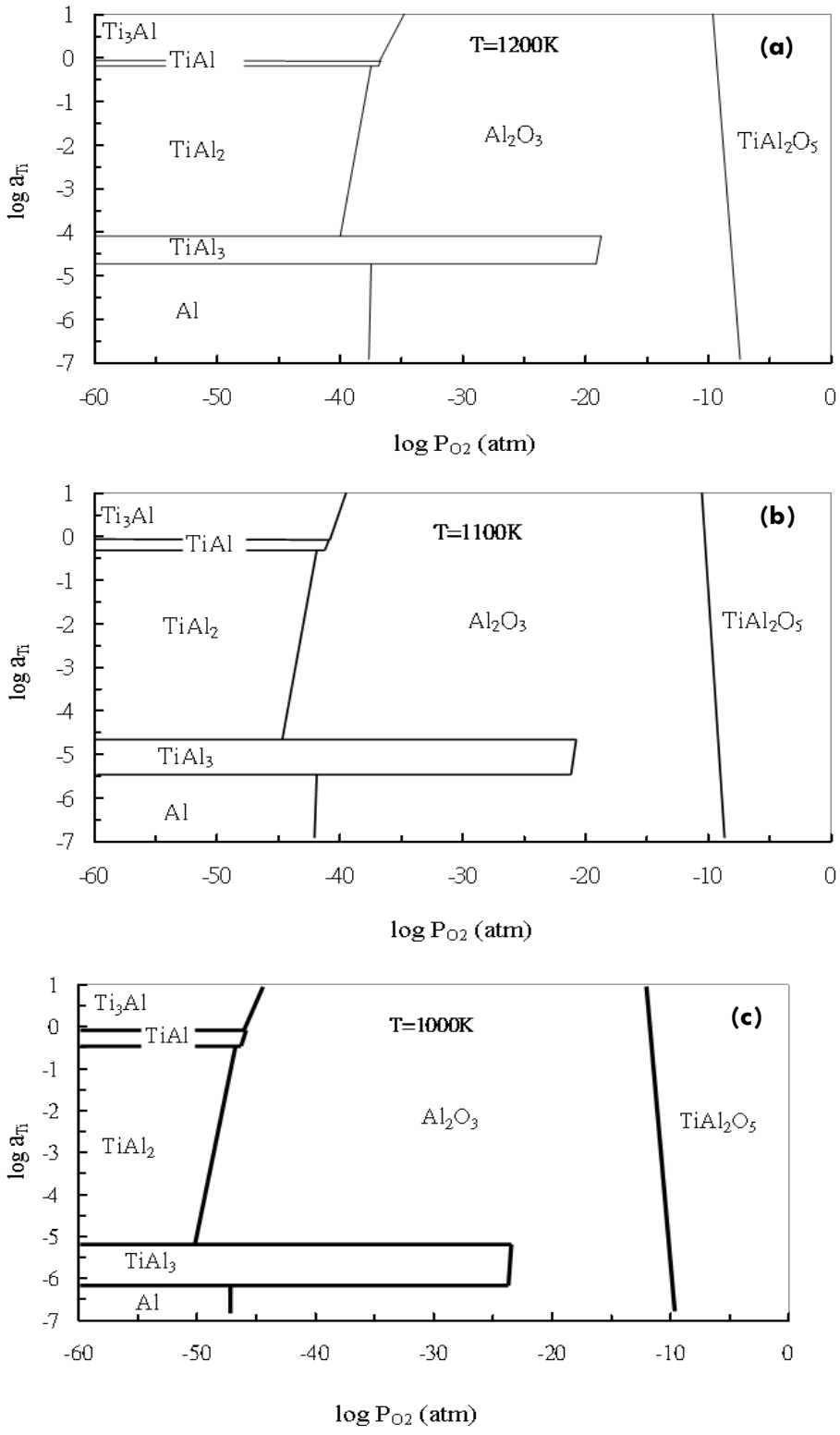

Figure 5. Condensed phases of Ti–Al–O compound regions on the log a_{TiO2} – log P_{O2} diagram in Ti–Al–O isothermal stability diagram at (a) 1000 K, (b) 1100 K, and (c) 1200 K.

Table 2. Reactions, equilibrium constant (*K*), and formation-Gibbs free energies (ΔG_f) of twelve possible compounds forming at Ti–Ai interface under oxygen pressure at a temperature range of 1000 to 1200 K.

No.	Eqn. Reactions	log *K*	ΔGf (kJ/mol)
1	$Ti_{(s)} + \frac{1}{2}O_{2(g)} \rightarrow TiO_{(s)}$	$-4.97 + \frac{28262.2}{T}$	$-541.1 + 0.09T$
2	$2Ti_{(s)} + \frac{3}{2}O_{2(g)} \rightarrow Ti_2O_{3(s)}$	$-14.14 + \frac{78926.6}{T}$	$-1511.2 + 0.271T$
3	$3Ti_{(s)} + \frac{5}{2}O_{2(g)} \rightarrow Ti_3O_{5(s)}$	$-23.72 + \frac{127944.3}{T}$	$-2449.7 + 0.452T$
4	$4Ti_{(s)} + \frac{7}{2}O_{2(g)} \rightarrow Ti_4O_{7(s)}$	$-32.16 + \frac{177194.3}{T}$	$-3392.7 + 0.621T$
5	$Ti_{(s)} + O_{2(g)} \rightarrow TiO_{2(s)}$	$-9.28 + \frac{49113.4}{T}$	$-940.4 + 0.181T$
6	$Ti_{(s)} + 2Al_{(l)} + \frac{5}{2}O_{2(g)} \rightarrow TiAl_2O_{5(s)}$	$-26.0 + \frac{137873.5}{T}$	$-2640.1 + 0.500T$
7	$2Al_{(l)} + \frac{3}{2}O_{2(g)} \rightarrow Al_2O_{3(s)}$	$-17.29 + \frac{88395.7}{T}$	$-1692.5 + 0.33T$
8	$3Ti_{(s)} + Al_{(l)} \rightarrow Ti_3Al_{(s)}$	$-0.35 + \frac{1547.7}{T}$	$-29.6 + 0.007T$
9	$Ti_{(s)} + Al_{(l)} \rightarrow TiAl_{(s)}$	$-0.88 + \frac{1955.7}{T}$	$-37.5 + 0.017T$
10	$Ti_{(s)} + 2Al_{(l)} \rightarrow TiAl_{2(s)}$	$-0.58 + \frac{2290.6}{T}$	$-43.9 + 0.011T$
11	$2Ti_{(s)} + 5Al_{(l)} \rightarrow Ti_2Al_{5(s)}$	$\log K = -2.87 + \frac{3797}{T}$	$-34.4 + 0.055T$
12	$Ti_{(s)} + 3Al_{(l)} \rightarrow TiAl_{3(s)}$	$\log K = -1.33 + \frac{9653}{T}$	$-40.3 + 0.010T$

Table 3. Eleven coexistence terms of reaction and Gibbs free energies of Ti–Al–O system on bivariant equilibria lines in a temperature range of 1000 to 1200 K.

No.	Interface	Reaction	*log K*	Equation
1	Al/Al_2O_3	$2Al_{(l)} + \frac{3}{2}O_{2(g)} \rightarrow Al_2O_{3(\alpha(}$	$-17.29 + \frac{88396}{T}$	$\log P_{O_2} = \frac{-2}{3}\log K$
2	$Al/TiAl_3$	$3Al_{(l)} + Ti \rightarrow TiAl_{3(s)}$	$-1.33 + \frac{9653}{T}$	$\log a_{Ti} = -\log K$
3	$TiAl_3/Ti_2Al_5$	$\frac{5}{3}TiAl_{3(s)} + \frac{1}{3}Ti \rightarrow Ti_2Al_{5(s)}$	$4.68 - \frac{2265}{T}$	$\log a_{Ti} = -3\log K$
4	$Ti_2Al_5/TiAl_2$	$\frac{5}{2}TiAl_{2(s)} \rightarrow \frac{1}{2}Ti + Ti_2Al_{5(s)}$	$-1.42 - \frac{1930}{T}$	$\log a_{Ti} = 2\log K$
5	$TiAl_2/TiAl$	$2TiAl_{(s)} \rightarrow TiAl_{2(s)} + Ti$	$1.18 - \frac{1621}{T}$	$\log a_{Ti} = \log K$
6	$TiAl/Ti_3Al$	$TiAl_{(s)} + 2Ti \rightarrow Ti_3Al_{(s)}$	$0.527 - \frac{408}{T}$	$\log a_{Ti} = \frac{-1}{2}\log K$
7	$Al_2O_3/TiAl_3$	$\frac{3}{2}Al_2O_{3(\alpha\alpha} + Ti \rightarrow \frac{9}{2}O_{2(g)} + TiAl_{3(s)}$	$22.6 - \frac{122941}{T}$	$\log P_{O_2} = \frac{2}{9}(\log K + \log a_{Ti})$
8	$Al_2O_3/TiAl_2$	$Al_2O_{3(\alpha\alpha} + Ti \rightarrow \frac{3}{2}O_{2(g)} + TiAl_{2(s)}$	$16.15 - \frac{86440}{T}$	$\log P_{O_2} = \frac{2}{3}(\log a_{Ti} + \log K)$
9	$Al_2O_3/TiAl$	$\frac{1}{2}Al_2O_{3(\alpha\alpha} + Ti \rightarrow \frac{3}{4}O_{2(g)} + TiAl_{(s)}$	$7.77 - \frac{42242}{T}$	$\log P_{O_2} = \frac{4}{3}(\log K + \log a_{Ti})$
10	Al_2O_3/Ti_3Al	$\frac{1}{2}Al_2O_{3(\alpha(} + 3Ti \rightarrow \frac{3}{4}O_{2(g)} + Ti_3Al_{(s)}$	$8.12 - \frac{42650}{T}$	$\log P_{O_2} = \frac{4}{3}(\log K + 3\log a_{Ti})$
11	$Al_2O_3/TiAl_2O_5$	$Al_2O_{3(\alpha(} + Ti + \frac{7}{2}O_{2(g)} \rightarrow TiAl_2O_{5(s)}$	$-8.71 + \frac{49478}{T}$	$\log P_{O_2} = \frac{-2}{7}(\log K + \log a_{Ti})$

The relationships between the vapor pressures and are:

$$\log K_2 = \log P_{Ti} \quad (10)$$

$$\log K_3 = \log P_{TiO} \quad (11)$$

$$\log K_4 = 3\log P_{TiO} + \log P_{O_2} \quad (12)$$

$$\log K_5 = 4\log P_{TiO} + \frac{3}{2}\log P_{O_2} \quad (13)$$

$$\log K_6 = \log P_{TiO} + \frac{1}{2}\log P_{O_2} \quad (14)$$

The partial pressure of $Ti_{(g)}$ and $TiO_{(g)}$ dominates the condensed phases $Ti_{(s)}$, $TiO_{(s)}$, $Ti_3O_{5(s)}$, $Ti_4O_{7(s)}$, and $TiO_{2(s)}$, as shown in Figure 2. Figures 3(a) and 3(b) also show that belted and stepped curves of $Ti_{(g)}$ and $TiO_{(g)}$ dominate the condensed phases $Ti_{(s)}$, $TiO_{(s)}$, $Ti_3O_{5(s)}$, $Ti_4O_{7(s)}$, and $TiO_{2(s)}$ in a temperature range of 900 to 1200 K, based on the results in Table 2.

Condensed Phases

Seven condensed phases ($Al_{(l)}$, $TiAl_{3(s)}$, $Ti_2Al_{5(s)}$, $TiAl_{2(s)}$, $TiAl_{(s)}$, $Ti_3Al_{(s)}$, and $Al_2O_{3(\alpha)}$) can be arranged on a (log P_{O2} – log α_{Ti}) diagram of the Ti-Al-O system at constant temperature. Figure 4 depicts the regions of each condensed phase along the axis in the (log P_{O2} – log α_{Ti}) diagram. This so-called isothermal stability diagram is useful in estimating the relationships between each pair of condensed phases in the Ti-Al-O system; however, the interfaces between each pair of phases cannot be clearly determined from the schematic diagram. Since multiple phases can accumulate at an interface, 35 assemblies can possibly be constructed in the $O_{(g)}$, $Ti_{(s)}$, $Al_{(l)}$, $TiAl_{3(s)}$, $TiAl_{2(s)}$, $TiAl_{(s)}$, $TiAl_2O_5$, $Ti_3Al_{(s)}$, and Al_2O_3 phases, namely Al/Al_2O_3, Al/TiO_2, $Al/TiAl$, $Al/TiAl_2$, $Al/TiAl_3$, Al/Ti_2Al_5, Al/Ti_3Al, $Al/TiAl_2O_5$, Al_2O_3/TiO_2, $Al_2O_3/TiAl$, $Al_2O_3/TiAl_2$, $Al_2O_3/TiAl_3$, Al_2O_3/Ti_2Al_5, Al_2O_3/Ti_3Al, $Al_2O_3/TiAl_2O_5$, $TiO_2/TiAl$, $TiO_2/TiAl_2$, $TiO_2/TiAl_3$, TiO_2/Ti_2Al_5, TiO_2/Ti_3Al, $TiO_2/TiAl_2O_5$, $TiAl/TiAl_2$, $TiAl/TiAl_3$, $TiAl/Ti_2Al_5$, $TiAl/Ti_3Al$, $TiAl/TiAl_2O_5$, $TiAl_2/TiAl_3$, $TiAl_2/Ti_2Al_5$, $TiAl_2/Ti_3Al$, $TiAl_2/TiAl_2O_5$, $Ti_2Al_5/TiAl_2O_5$, Ti_2Al_5/Ti_3Al, $TiAl_3/Ti_3Al$, $TiAl_3/TiAl_2O_5$, and $Ti_3Al/TiAl_2O_5$.

However, as shown in Figure 4, no interfaces of $Al/TiAl_3$, $Al/TiAl$, Al/Ti_3Al, $TiAl_3/TiAl_2$, $TiAl_3/TiAl$, $TiAl_3/Ti_3Al$, or $TiAl_2/Ti_3Al$ are found. Therefore, there are 35 terms, except those associated with these ten non-existing interfaces, are present, as shown in Figure 4. Nevertheless, there is still a problem of overlapping

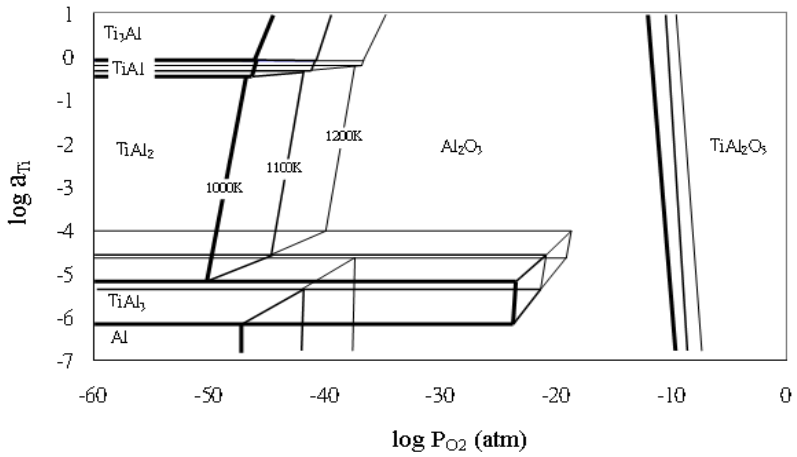

Figure 6. Isothermal stability diagram of Ti-Al-O compounds in a temperature range of 1000 to 1200 K under various oxygen pressures and Ti activity values.

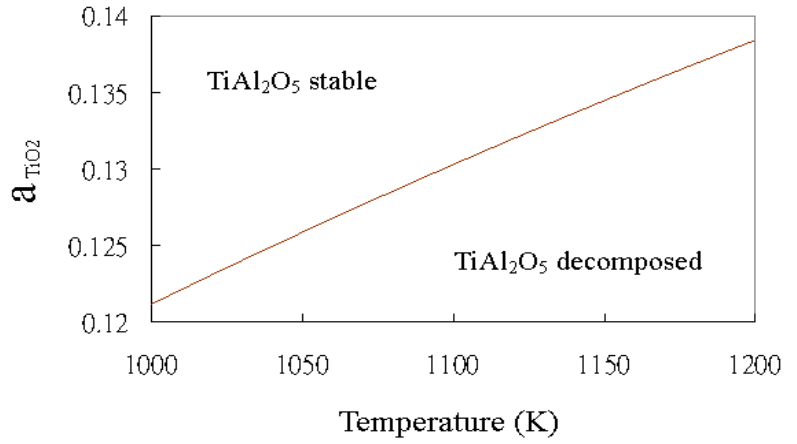

Figure 7. Decomposition curve of spinel ($TiAl_2O_5$) with varying TiO_2 activity from 1000 to 1200 K.

in the Al_2O_3 and $TiAl_2O_5$ regions. Thus, several other interfaces should not exist and therefore should be removed from the 35 terms. The interfaces $Al/TiAl_2O_5$, $Al/TiAl_3$, $Al/TiAl_2$, Al/TiAl, and Al/Ti_3Al must be omitted to label the compound's domains in Figure 4. Finally, only ten coexisting terms were retained from the original terms. Table 3 presents the equations and obtained Gibbs free energy of the ten coexistent terms. Combining Figure 4 with the thermodynamic data from Table 3 yields the interfaces of compounds, as presented in Figure 5.

For example, to estimate the boundaries of the TiAl region, firstly, reactions 15, 16, 17, and 18, and their Gibbs free energy of formation are obtained from Table 2. Secondly, the relationship between the activity of Ti and the oxygen partial pressure is obtained from reaction 15, under the $TiAl/Al_2O_3$ coexistence condition. Thirdly, the activity of Ti is calculated from reaction16 under the $TiAl/TiAl_2$ coexistence condition. Finally, reaction 17 can also be used to calculate the activity of Ti under the $TiAl/Ti_3Al$ coexistence condition,

$$\frac{1}{2}Al_2O_{3(\alpha)} + Ti_{(s)} \rightarrow \frac{3}{4}O_{2(g)} + TiAl_{(s)} \quad (15)$$

$$2TiAl_{(s)} \rightarrow TiAl_{2(s)} + Ti_{(s)} \quad (16)$$

$$TiAl_{(s)} + 2Ti_{(s)} \rightarrow Ti_3Al_{(s)} \quad (17)$$

Additionally, the oxygen pressure obtained from reaction 15 is:

$$\log P_{O_2} = \frac{4}{3}(\log K + \log a_{Ti}) \quad (18)$$

The oblique line in Figure 5 drawn along the axis in the log P_{O2} – log a_{Ti} diagram represents the interface between Al_2O_3 and TiAl. The activity of Ti between TiAl and $TiAl_2$ can be determined from reaction 16 as follows:

$$\log a_{Ti} = \log K \quad (19)$$

Therefore, in Figure 5, one horizontal line (the interface between TiAl and $TiAl_2$) is determined by reaction 19, and the other horizontal line (the interface between TiAl and Ti_3Al) is determined from reaction 17; the three lines define the TiAl region. Accordingly, in Figure 5, the regions associated with the other compounds can also be determined, and then the equations of univariant equilibria (triple-phase coexistence) points can be calculated, as shown in Table 3. Furthermore, overlapping Figures 5 (a), (b), and (c) produces a 3-D (axes temperature, log P_{O2} – log a_{Ti}) isothermal stability diagram, as presented in Figure

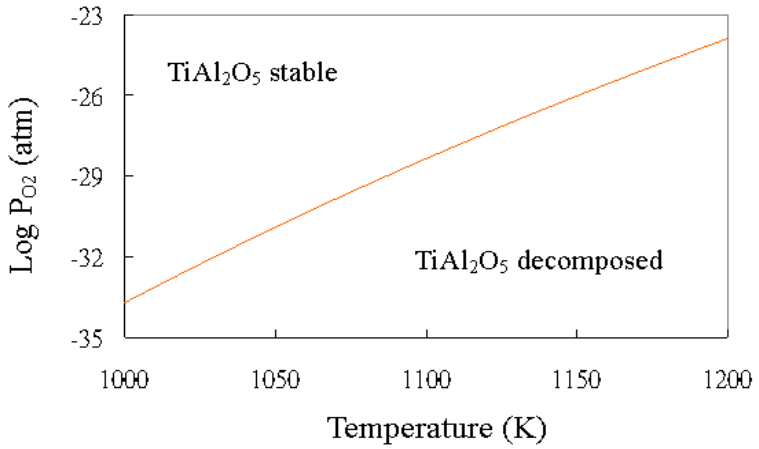

Figure 8. Decomposition curve of spinel ($TiAl_2O_5$) with varying partial pressure of oxygen from 1000 to 1200 K.

6. The temperature range is widened from 1000 to 1200 K. The diagram clearly shows regions for Al, Al_2O_3, $TiAl_3$, $TiAl_3$, Ti_3Al_5, TiAl, Ti_3Al, and $TiAl_2O_5$ at various temperatures.

Discussion

Sorting Compounds by Gibbs Free Energy of Formation

The thermodynamic stabilities of compounds in a Ti-Al-O system were evaluated by considering their Gibbs free energy, based on the data in Table 2. In a Ti-Al-O system, in ascending order of Gibbs free energy, the compounds at 1000 K are: $Ti_4O_{7(s)} \rightarrow TiAl_2O_{5(s)} \rightarrow Ti_3O_{5(\alpha)} \rightarrow Al_2O_{3(\alpha)} \rightarrow Ti_2O_{3(\alpha)} \rightarrow TiO_{2(s)} \rightarrow TiO_{(\alpha)} \rightarrow Ti_3Al_{(s)} \rightarrow TiAl_{2(s)} \rightarrow TiAl_{3(s)} \rightarrow Ti_2Al_{5(s)} \rightarrow TiAl_{(s)}$. Thus, $Ti_4O_{7(s)}$ is the most stable phase, and TiAl(s) is the least stable compound. In conclusion, the order of formation of Ti-Al-O intermetallic compounds can be determined from thermodynamics. The Ti3Al(s) phase is the first to appear, but the TiAl phase is the last to appear.

Equations for Spinel Formation

Four different equations for the formation of spinel are,

$$TiO_{2(s)} + Al_2O_{3(\alpha(} \rightarrow TiAl_2O_{5(s)}, \quad (\Delta G = -7.2 - 0.011T\ (\text{kJ/mol})) \quad (20)$$

$$Ti_{(s)} + \frac{5}{3}Al_2O_{3(\alpha(} \rightarrow TiAl_2O_{5(s)} + \frac{4}{3}Al_{(l)}, (\Delta G = 180.73 - 0.05T\ (\text{kJ/mol})) \quad (21)$$

$$2Al_{(l)} + TiO_{2(s)} + \frac{3}{2}O_{2(g)} \rightarrow TiAl_2O_{5(s)}, \quad (\Delta G = -1700.1 + 0.32T\ (\text{kJ/mol}) \quad (22)$$

$$Ti_{(s)} + 2Al_{(l)} + \frac{5}{2}O_{(g)} \rightarrow TiAl_2O_{5(s)}, \quad (\Delta G = -2640.1 + 0.5T\ (\text{kJ/mol})) \quad (23)$$

Reaction 20 is a general form of the spinel forming equation in the phase diagram of Figure 1(d). Moreover, its Gibbs free energy of formation of the spinel is less than zero (-18.2 kJ/mol at 1000 K), so the reaction is possible to form the spinel. However, the Gibbs free energy of reaction 21 is too high (130.73 kJ/mol at 1000 K). Hence, this equation cannot describe the formation of the spinel. Despite the fact that the Gibbs free energy of reaction 22 is negative and low (-1380.1 kJ/mol at 1000 K), it is an impossible equation, since the partial pressure of oxygen at which alumina is formed (10-47.4 atm at 1000 K) and the Gibbs free energy (-1380.1 kJ/mol at 1000 K) of the formation of alumina are lower than those in TiO_2 (10-39.8 atm at 1000 K). Therefore, at the Al/TiO_2 interface, Al_2O_3 may form when TiO_2 decomposes at high temperature. In other words, if Al oxidizes to Al_2O_3 first, the reaction becomes that described by reaction 23, in which the Gibbs free energy (2140.1 kJ/mol at 1000 K) is lower than that of reaction 22. Therefore, reaction 23 is more possible than reaction 22. With reference to reaction 20, the oxygen partial pressures of the decomposition of Al_2O_3 and TiO_2 at 1000 K are 10-47.4 and 10-39.8 atm, respectively, according to Table 2. If the partial pressure of oxygen in the system is between 10-47.4 and 10-39.8 atm, Al oxidizes to alumina, and Ti does not oxidize to TiO_2. Therefore, reaction 23 is possible.

Ti-Al Intermetallic Compounds

In the general form of the spinel forming equation in the phase diagram of Figure 1(d), the reaction 21 has log K = 0.57 + 364.6/T, and the activity of TiO_2 is expressed with log a_{TiO2} = – log K when the activity of Al_2O_3 is unity. The activity of TiO_2 controls the stability of $TiAl_2O_5$. For example, Figure 7 shows that when activity of TiO_2 is less than 0.121 at 1000 K, $TiAl_2O_5$ will be decomposed. The partial pressure of O_2 also controls the stability of $TiAl_2O_5$, the reaction being as 22. For example, Figure 8 shows that when the activity of Al is unity, log a_{TiO2} = -0.57 – 364.6/T, and log P_{O2} is less than –33.7 atm at 1000 K, $TiAl_2O_5$ will be decomposed. In Figures 7 and 8, when a_{TiO2} < 0.121 and –33.7 > log P_{O2} > 39.8 atm at 1000 K, both $TiAl_2O_5$ and TiO_2 are stable. In contrast, when a_{TiO2} < 0.121 and log P_{O2} < 39.8 atm at 1000 K, $TiAl_2O_5$ is decomposed; when and at 1000 K, both $TiAl_2O_5$ and TiO_2 are decomposed. Various elements and compounds presented in the Ti-Al interfaces depend on a_{TiO2} and P_{O2} conditions at various temperatures, such that high temperature, low oxygen pressure, and low TiO_2 activity are the possible conditions for obtaining $Ti_3Al_{(s)}$, $TiAl_{2(s)}$, $TiAl_{3(s)}$, $Ti_2Al_{5(s)}$, and TiAl phases.

Conclusions

Thermodynamic calculations were performed to estimate Ti/Al interface reactions under various partial oxygen pressures and the activities of titanium conditions in the Ti-Al-O system. Solid, liquid, and gas phases in the Ti-Al-O system were analyzed using thermochemical data and phase diagrams. Seven condensed phases ($Al_{(l)}$, $Al_2O_{3(s)}$, $TiAl_{3(s)}$, $TiAl_{2(s)}$, $TiAl_{(s)}$, $Ti_3Al_{(s)}$, and $TiAl_2O_{5(s)}$) were arranged along an axis of a 3-domain diagram. The oxides forming in the Ti/Al interface were dependent on the temperature, activity of TiO_2, and partial oxygen pressure. When $a_{TiO2} > 0.121$ and log $P_{O2} > -33.7$ atm at 1000 K, both $TiAl_2O_5$ and TiO_2 are stable. On the contrary, when and at 1000 K, both $TiAl_2O_5$ and TiO_2 were decomposed in the Ti/Al interfaces. A 3-D diagram of Ti-Al-O isothermal stability was constructed over the temperature range of 1000 to 1200 K. This diagram is useful for determining accurate areas of $TiAl_2O_5$, Al, Al_2O_3 and Ti/Al intermetallic compounds in the Ti-Al-O system. In Ti/Al systems, TiAl and Ti_3Al have favorable properties at elevated temperatures. According to thermodynamic calculations, low oxygen pressure, high temperature, and low TiO_2 activity promote the formation of TiAl and Ti_3Al phases.

Acknowledgements

This work was financially supported by the Chung-Shan Institute of Science and Technology (CSIST) under the Contract No. CSIST-442-V103, and NSC 102-2221-E-239-008.

References

Barin I (1989) Thermochemical Data of Pure Substances. VCH verrlagsgesellschaft mbh, New York, USA, pp.17, 18, 45-48, 1520, 1521, 1544-1550.

Braun J, and M Ellner (2001) Phase equilibria investigations on the aluminum-rich part of the binary system Ti-Al. Metall Mater Trans A 32 (5): 1037-1047.

Cai ZH, DL Zhang (2006) Sintering behaviour and microstructures of Ti(Al,O)/Al_2O_3, Ti_3Al(O)/Al_2O_3 and TiAl(O)/Al_2O_3 in situ composites. Mater Sci Eng A 419 (1-2): 310-317.

Caron M, G Gagnon, V Fortin, JF. Currie, L Ouellet,Y Tremblay, M Biberger, and R Reynolds (1996) Calculation of a Al–Ti–O–N quaternary isotherm diagram for the prediction of stable phases in TiN/Al alloy contact metallization. J Appl Phys 79 (8): 4468-4473.

Charlu TV, OJ Kleppa, and TB Reed (1974) High-temperature combustion calorimetry III. Enthalpies of formation of titanium oxides. J Chem Thermodynamics 6 (11): 1065-1074.

Chase MW Jr., CA Davies, JR Downey, Jr. DJ Furip, RA McDonald, and AN Syverud (1985) JANAF Thermochemical Tables Third Edition. American Chemical Society, New York, USA, pp. 1679-1684.

Chen YL, M Yan, YM Sun, BC Mei, and JQ Zhu (2009) The phase transformation and microstructure of TiAl/Ti_2AlC composites caused by hot pressing. Ceram Inter 35 (5): 1807-1812.

Chen Y, DJ Young, and B Gleeson (1995) A new Ti-rich ternary phase in the Ti-Al-O system. Mater Lett 22 (3-4): 125-129.

Cheng L, H Chang, B Tang, H Kou, and J Li (2013) Characteristics of metadynamic recrystallization of a high Nb containing TiAl alloy. Mater Lett 92 (1): 430-432.

Copland E (2006) Vapor pressures in the {$Al_{(l)}$ + $Al_2O_{3(s)}$} system: Reconsidering $Al_2O_{3(s)}$ condensation. J Chem Thermodynamics 38 (4): 443-449.

Dehm G, C Scheu, M Rühle, and R Raj (1998) Growth and structure of internal Cu/Al_2O_3 and Cu/Ti/Al_2O_3 interfaces. Acta Mater 436 (3): 759-772.

Feng ZS, JJ Chen, C Zhang, N Zhao, and Zi Liang (2012) Formation of Al_2O_3–TiO_2 composite oxide films on aluminum foil by cathodic electrodeposition and anodizing. Ceram Inter 38 (3): 2501-2505.

Gerasimov KB, and SV Pavlov (1996) Metastable Ti-Al phases obtained by mechanical alloying. J Alloys Compd 242 (1-2): 136-142.

Kainuma R, M Palm, and G. Inden (1994) Solid-phase equilibria in the Ti-rich part of the Ti–Al system. Intermetallics 2 (4): 321-332.

Kostov A, and D Živković (2008) Thermodynamic analysis of alloys Ti–Al, Ti–V, Al–V and Ti–Al–V. J Alloys Compd 460 (1-2): 164-171.

Kuo CG, WD Jehng, SJ Hsieh, and CC Chen (2009) Phase equilibria on Ni–Al interface under low oxygen pressure. J Alloys Compd 480 (2): 299-305.

Li XL, R Hillel, F Teyssandier, SK Choi, and FJJ. Van Loo (1992) Reactions and phase relations in the Ti-Al -O system. Acta Metall Mater 40 (11): 3149-3157.

Lin CK, SS Hong, and PY Lee (2000) Formation of NiAl–Al_2O_3 intermetallic-matrix composite powders by mechanical alloying technique. Intermetallics 8 (9-11): 1043-1048.

Lu H, CL Bao, DH Shen, XJ Zhang, YD Cui, and ZD Lin (1995a) Study of the Ti/Al_2O_3 interface. J Mater Sci 30 (2): 339-346.

Lu YC, SL Sass, Q Bai, DL Kohlstedt, and WW Gerberich (1995b) The influence of interfacial reactions on the fracture toughness of Ti/Al_2O_3 interfaces. Acta Metall Mater 43 (1): 31-41.

Pang JC, GH Fan, XP Cui, AB Li, L Geng, ZZ Zheng, and QW Wang (2013) Mechanical properties of Ti–(SiC_p/Al) laminated composite with nano-sized $TiAl_3$ interfacial layer synthesized by roll bonding. Mater Sci Eng A 582: 294-298.

Pourbaix M (1974) Atlas of Electrochemical Equilibria in Aqueous Solutions. National Association of Corrosion Engineers, Houston, USA, pp. 213-222.

Seifert HJ, A Kussmaul, and F Aldinger (2001) Phase equilibria and diffusion paths in the Ti–Al–O–N system. J Alloys Compd 317-318 (12): 19-25.

Wang L, JX Shang, FH Wang, Y Chen, and Y Zhang (2013) Oxygen adsorption on γ-TiAl surfaces and the related surface phase diagrams: A density-functional theory study. Acta Mater 61 (5): 1726-1738.

Ward-Close CM, R Minor, and PJ Doorbar (1995) Intermetallic-matrix composite – a review. Intermetallics 4 (3): 217-229.

Wriedt HA (1985) The Al-O (Aluminum-Oxygen) system. Bull. Alloy Phase Diagrams 6 (6): 548-553.

Xu L, YY Cui, YL Hao, and R. Yang (2006) Growth of intermetallic layer in multi-laminated Ti/Al diffusion couples. Mater Sci Eng A 435-436 (5): 638-647.

Zalar A, BMM Baretzky, S Hofmann, M Rühle, and P Panjan (1999) Interfacial reactions in Al_2O_3/Ti, Al_2O_3/Ti_3Al and Al_2O_3/TiAl bilayers. Thin Solid Films 352 (1-2): 151-155.

Zhong H, Y Yang, J Li, J Wang, T Zhang, S Li, and J Zhang (2012) Influence of oxygen on microstructure and phase transformation in high Nb containing TiAl alloys. Mater Lett 83 (1): 198-201.